

GIS-BASED CELL MODEL FOR SIMULATING DEBRIS FLOW ROUTING AND DEPOSITION PHASES ON A FAN

C. GREGORETTI^(*), M. FURLAN^(*) & M. DEGETTO^(*)

^(*) University of Padova - Dipartimento Territorio e Sistemi Agro-Forestali - Italy

ABSTRACT

A GIS-based cell model is proposed for the simulation of the routing and deposition phases of debris flow on a fan. Flow pattern is discretized by square cells, 2m size, which coincide with the DEM cells and the mixture is assumed a monophasic continuum. Flow exchange between adjacent cells is ruled by uniform flow or broad-crested weir laws and by continuity equation. Flow occurs from cells with higher surface to those with lower surface and is simulated by uniform flow law if the elevation of the formers is higher than the latter and by broad-crested weir law otherwise. Erosion and deposition are simulated using the empirical law of Egashira, adjusted for monophasic continuum. The cell model is used to simulate debris flow occurred on Rio Lazer (Dolomites, Eastern Italian Alps) the 4th of November 1966. The same event was also simulated using Flo-2D model for a comparison with a widely used model for debris flow simulation. Results of the two simulations were compared with extension of deposition area and the map of measured depths of deposited sediments. Both the model simulate quite well the extent of deposition area, whereas the deposited debris depths are better simulated by the cell model.

KEY WORDS: GIS, cell model, fan spreading, hazard map

INTRODUCTION

Debris flows in the Dolomites usually occur for the mobilization of sediment accumulated on the bed

of channels incising debris fan after the impact with runoff descending from the upstream cliffs. The routing path of debris flows is usually obliged and coincides with the channel in the upper part of the fan but in the medium part it can deviate (TAKANASHI *et alii*, 2007) and in the lower part, where terrain slope diminishes, can spread (IVERSON *et alii*, 1998; RICKENMAN, 2005; BERTI & SIMONI, 2007). Hazard mapping concerns the identification of the threatened area, historical or potential, by debris flows. Therefore hazard maps are built both using data from surveys of areas flooded by debris flows and through the simulation of potential scenarios. The models (methods) used for the simulation of a potential scenario are empirical (AULITZKY, 1973), empirical-statistical (BERTI & SIMONI, 2007; GRISWOLD & IVERSON, 2008; SCHEIDL & RICKENMAN, 2010), topographic gradient based (GRUBER, 2007), numerically based by integration of shallow water equations (BRUFAU *et alii*, 2000; ARMANINI *et alii*, 2009), SPH (PASTOR *et alii*, 2008) and automata cellular (DEANGELI & SEGRE, 1995; D'AMBROSIO, 2003, DEANGELI, 2008). In this work a GIS-based cell model is proposed. Cell model was proposed by ZANOBETTI *et alii*, (1970) for simulate flood inundation of rural area of large extension and was successively adapted to simulate flood and runoff routing in urban areas (RICCARDI, 1997; MASCARENHAS & MIGUEZ, 2002; MIGUEZ *et alii*, 2009; CHEN *et alii*, 2009). In these models cells are linked on the base of flow characteristics (channel flow, weir flow, floodplain flow). Moreover, a cell model was also used to simulate

soil erosion and sediment outflow from a catchment where flow paths to the outlet are, a priori, determined using topographic gradient and the routing is ruled by De Saint Venant equation without inertia terms (JAIN *et alii*, 2005). The proposed model does not distinguish the cells but the hydraulic links that depend on both the bottom and flow surface elevation between neighbouring cells and is not limited by the topographic gradient. The mathematical structure of the model is analogous to that used by cellular automata models and that of FLO-2D model even if the latter does not simulate the sediment entrainment and deposition.

THE CELL MODEL

OVERVIEW

The flow cell concept, as introduced by ZANOBETTI *et alii*, (1970), proposes to represent a basin through homogeneous compartments, channels, floodplain galleries, weirs which are in turn represented by cells. Each cell interacts with the neighbouring cell by hydraulic links (Saint Venant equations, with or without inertia terms, broad-crested weirs, orifices, gates laws) that are chosen on the base of the cell type: two “channel” cells interact using the De Saint Venant equation, a “channel” cell interacts with a “floodplain” cell by the weir equation, and so on. The cell model is able to reproduce multiple flow patterns as those of urban areas and overcomes the difficulty of implementing the usual numerical 2D models based on the shallow water equations in a complex environment of streets, buildings, elevated terrains and so on. On the other hand JAIN *et alii* (2005) used a cell model to route runoff and sediment to the outlet considering only a flow path departing from each cell along the steepest slope, that is, towards the surrounding cell of lowest altitude. The model proposed by JAIN *et alii* (2005) is therefore an hybrid between one and two-dimensional models, because for each cell the inflow could come from more than one of the neighbouring cells but the outflow is only to the lowest altitude cell. Moreover, this technique needs the pre-processing of DEM at the purpose to eliminate holes that can interrupt the flow path between a cell and the outlet.

In the case of debris flows, as the case of urban areas, the usual dam-break two-dimensional models which integrate the shallow water equations, meet some difficulties that are due to the irregular and sloping flow pattern and the presence of civil structures. On the other hand the distributed cell model considering



Fig. 1 - Scheme of the possible flow directions

only one flow direction, that conveys flow towards the more depressed cell is inadequate to simulate debris flow spreading in the deposition areas. Objective of this paper is a robust model based on strong simplification of hydraulics (i.e. flow cell) that allows a reliable simulation of routed areas and sediment deposits of debris flow. In this work the flow cell is used to simulate the debris flow routing and deposition phases on a fan and the flow cell scheme of ZANOBETTI *et alii* (1970) is therefore adapted to debris flow spreading on a fan using two hydraulic links to simulate flow exchange of a cell with the neighbours. Flow occurs from cell with higher flow surface elevation towards cell with lower surface elevation and is simulated by the uniform flow equation in the case of flow from higher elevation cell to lower elevation cell and by the weir equation otherwise.

Flow patterns is discretized using pixel of the DEM and flow exchange between cells is computed by uniform flow and weir equation laws, requiring the respect of continuity equation. The governing equations, then, are those of continuity for each cell and discharge relationships between linked cells. Eight possible flow directions are assumed (Figure 1) as in the FLO-2D model and a possible lattice geometry in automata cellular models (SEGRE & DEANGELI, 1995).

Basic assumptions of the model are summarized as follows:

1. The solid-liquid mixture is assumed continuum and monophasic;
2. Exchange flow relationship between adjacent cells are uniform flow and broad-crested weir equations;
3. The cell flow surface is considered horizontal;
4. There are eight possible flow directions;
5. Flow section between cells are considered rectangular;
6. Flow volume inside cell is function of the flow depth;
7. Exchange flow of a cell with the neighbouring ones is simultaneous;
8. The discharge exchanged between neighbouring cells depends on the flow levels of the cells.
9. The computation method is explicit and the time step is computed using the CFL condition.

CONTINUITY EQUATION

Two basic assumptions of continuity equation are: a) the flow volume V_i^t in the cell i at time t is obtained multiplying the corresponding flow depth at time t , h_i^t , by the cell area; b) the exchanged discharge at time step $n\Delta t$ ($t = (n-1)\Delta t$) depends on the flow depths of cells. In differential form, the continuity equations is:

$$A \frac{dh_i}{dt} = Ai_{b,i} - \sum_{k=1}^8 Q_{i,k} \tag{1}$$

where A = cell area; $i_{b,i}$ is the bed erosion/deposition velocity; $Q_{i,k}$ is the discharge exchanged between cell i and k and is assumed positive if directed towards cell k , negative otherwise.

DISCHARGE EXCHANGE RELATIONSHIP BETWEEN CELLS

There are two types of exchange relationships between a cell and those surroundings with lower flow elevation: uniform flow equation if cell elevation is higher than that of the surrounding one (Figure 2a); modified broad-crested equations if cell elevation is lower than that of the surrounding one (Figure 2b). The discharge equations in the two case are respectively:

$$Q_{i,k} = C h_i \Delta x w_{i,k} \sqrt{gh_i \sin \vartheta_{i,k}} \tag{2}$$

$$Q_{i,k} = 0.385 \Delta x s_{i,k} \sqrt{2g(h_i - h_k)^{1.5}} \tag{3}$$

where C is the conductance coefficient (TSUBAKI, 1972); Δx is cell size; $\vartheta_{i,k}$ is the angle respect to the horizontal between the line joining the centres of cell i and k ($\text{atan}(z_i - z_k)/\Delta x$); z_i is the bottom elevation of cell; $w_{i,k}$ e $s_{i,k}$ are two weighting functions:

$$w_{i,k} = \frac{\sin \vartheta_{i,k}}{\sum_{\kappa=1}^v \sin \vartheta_{i,\kappa}} \tag{4}$$

$$s_{i,k} = \frac{h_i - h_k}{\sum_{k=1}^m h_i - h_k} \tag{5}$$

where n and m are the number of surrounding cells for which $\sin \vartheta_{i,k}$ and $h_i - h_k$ are positive. The broad-crested equation has been modified considering the difference between flow surface elevations of the two cells instead of the difference $h_i - z_k$. This modification holds the larger energy loss due to the presence of sediments and should avoid the use of a diminution discharge coefficient in the case of drowned “weir”. The weighting functions depend on the topographic and flow surface drops respectively and are used to narrow the flow width because of the flow is not one-dimensional.

EROSION AND DEPOSITION

Erosion and deposition are modelled through the empirical equation of EGASHIRA & ASHIDA (1987) which is converted for a continuum mono-phase:

$$i_{b,i} = K \sum_{i=1}^{m+n} U_{i,k} (\sin \vartheta_{i,k} - \sin \vartheta_{LIM}) \tag{6}$$

where K is an empirical constant between 0 and 1; $U_{i,k}$ is the mean velocity corresponding to the discharge $Q_{i,k}$; $\vartheta_{i,k}$ is the angle respect to the horizontal between the line joining the centres of the cells i and k in the case of uniform flow and the angle between the line joining the centres of flow surfaces of cell i and k diminished of the adverse topographic slope between the two cells in the case of weir flow; ϑ_{LIM} is the limit angle for both erosion and deposition (it assume different values for erosion and deposition respectively: ϑ_{LIM-E} and ϑ_{LIM-D}). Erosion occurs for $\vartheta_{i,k} > \vartheta_{LIM-E}$ and $U_{i,k} > U_{LIM-E}$, being U_{LIM-E} the limit inferior value of mean velocity for erosion. Deposition occurs for $\vartheta_{i,k} < \vartheta_{LIM-D}$ and $U_{i,k} < U_{LIM-D}$, being U_{LIM-D} the limit superior value of mean velocity for deposition.

ALGORITHM STRUCTURE

Dem cells are divided into two classes: boundary cells where the input hydrograph is inserted (input

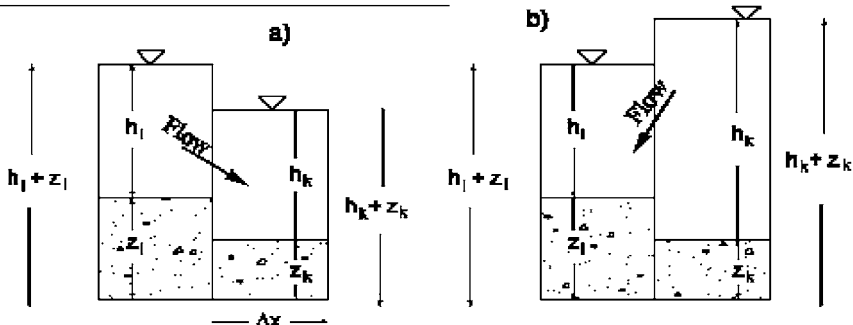


Fig. 2 - Scheme of the possible flow between two adjacent cells

boundary cells) or there is outflow (output boundary cells) and routing cells. At the first time step, only the input boundary cells are activated by filling it with the volume of the input hydrograph corresponding to the first time step. At the second time step, flow routing from input boundary cells towards those surroundings occurs. At the third time step, flow routing occurs from input boundary cells and those surroundings and from the cells routed at the previous time step towards those surrounding the last ones. The coordinates of cells routed for the first time during a same time step are stored in a vector. So at each time step corresponds a vector containing the coordinate of activated cells, that is those routed for the first time. Flow routing is computed sequentially from the input boundary cells followed from the first order routed cells (cells routed at the second time step) and so on. Input boundary cells cannot be routed by other cells but receive flow only by the input hydrograph and are not subjected to erosion and deposition. The time step is computed according to the CFL condition with the Courant number equal to 0.95. This last constraint does not origin from numerical instabilities problems but is used at the purpose of respecting the physics of routing. The numerical scheme is explicit, that is the quantity at the time $t + \Delta t$ is computed by the values of the quantities at time t . Therefore, equation (1) after the integration in time, for the generic cell i , becomes:

$$h_i^{t+\Delta t} = h_i^t + \left[i_{b,i}^t - \frac{1}{A} \sum_{k=1}^8 Q_{i,k}^t \right] \Delta t \quad (7)$$

The computation procedure is as it follows: for each cell the possible flow discharges versus the surroundings cells are computed according to equations (2) and (3); once all the flow discharges are computed the cell outflow volume is checked and in the case it results lower than the cell flow volume at the beginning of the time step, all the flow discharges are proportionally diminished to obtain the equality between outflow volume and flow volume of the cell at the beginning of time step. For each cell, then, the erosion bed velocities corresponding to the flow discharges are computed and summed according to equation (6). Positive value of $i_{b,i}$ means erosion and a negative value, deposition. If the product $A i_{b,i} \Delta t$ in the case $i_{b,i} < 0$ (deposition), results larger than the difference between flow cell volume at the beginning of time step and the outflow volume computed for the present time step, it is assumed a deposited volume equal to the difference

between these volumes. After computing the outflow volumes of all the cells and the corresponding bed erosion/deposition velocities, flow surface elevations of all the cells are simultaneously updated summing, for each cell, the outflow, inflow, deposited and eroded volumes just computed. The output boundary cells exchange flow discharge both with the surrounding cells and with the extern. The flow exchange with the extern is simulated without weighting functions by equations (2) and (3) along flow directions by which the boundary cell receives flow discharges according to uniform flow and broad-crested weir equations respectively. In other words, the flow directions from the boundary cell toward the extern coincide with those from inner cells to the boundary cell. Moreover there are other two parameters hROUT and hER. The first, hROUT, is the minimum flow depth for routing to avoid the routing of very small flow depth (inferior to 0.01 m) that is a physical non sense. This parameter is somehow comparable to the roughness height. The second, hER, is analogous to the previous one and is a lower bound for the flow erosion capacity. At the end of the simulation flow depths inferior to hROUT are assumed deposited.

The simultaneous updating of flow surface elevation for all the cells approaches the parallelization technique used in the cellular automata models. On the base of that written above there is a strong similarity between this cell model and cellular automata models. In fact this model corresponds to a cellular automata model without substates with local rules given by equations (1), (2) and (3) and mobilisation condition given by flow level larger than that in the surrounding cells and a flow depth larger than h_{ROUT} .

RIO LAZER BASIN AND DEBRIS FLOW OCCURRED THE 4TH OF NOVEMBER 1966

Rio Lazer basin is located in the Trento province (Dolomites, North Eastern Italy) with the largest altitude equal to 1608 m a.s.l.. Its extension is 1.57 km² and the average slope 30.8 %. Rio Lazer torrent origins at 1200 m a.s.l. and joins Cismon torrent at 742 m a.s.l. between the built-up areas of Siror and Tonadico (figure 3). The 4th of November 1966 a debris flow initiated at 850 m a.s.l. after high intensity rainfall and routed along the main channel. Just downstream the wooded area (figure 3), it spilled out the channel and flooded the entire fan depositing sediments of about 80800 m³ volume (computed associating a deposition depth d to the four deposi-



Fig. 3 - Aerial photo of Rio Lazer flooded area with superimposed the sediment deposits maps and the DEM contour

tion depth intervals of figure 3 that is equal to 0.05, 0.3, 0.75 and 1.5 m respectively). Most of deposited sediment (70686 m³) are in the area where d is larger than 0.5 m.

Figure 3 shows the aerial photo of the lower part of the basin with superimposed the contour of DEM that was built (pixel size 2 m) and the deposit map. The digital elevation model was built on the base of 3000 topographic measurements covering an area of 0.2 km². The input hydrograph was built combining the measured volume of deposited sediments with the runoff computed by an hydrological model. The total volume is 93900 m³ that corresponds to a sediment concentration equal to 0.86. The inlet cells where the hydrograph is entered are ten and located in the upper part of the watershed (the input hydrograph is distributed over a 20 m length). Therefore the total volume is equally divided for 10 and assigned to each of the hydrograph of the ten cells and is showed in figure 4.

FLO-2D SIMULATIONS

The scenario of debris flow occurred on Rio Lazer was simulated as a mudflow because FLO-2D cannot simulate erosion or deposition for the grain-inertial behaviour of mixture. Simulations were carried out using the values of parameters of the rheological quadratic law given by O' Brien and Julien (1985) corresponding to Aspen Natural Soil (Flo-2D user manual) which allowed the best reconstruction of the occurred event. In this case the sediment concentration was assumed equal to 0.45 instead of 0.86 that causes the deposition of most of sediments in the upper part of the watershed.

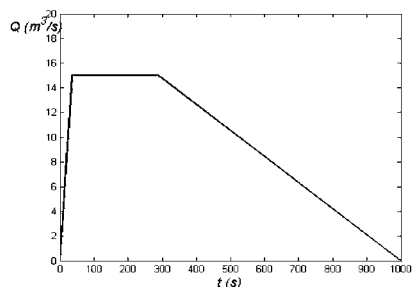


Fig. 4 - Reconstructed hydrograph for each of the ten inlet cells

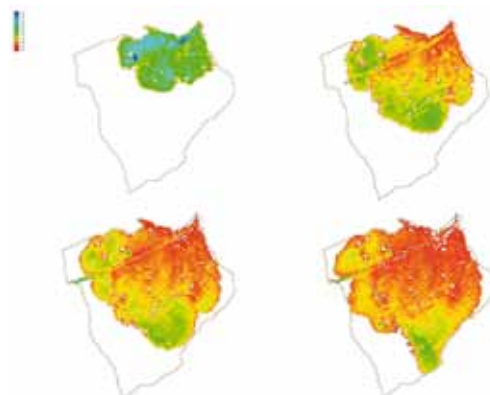


Fig. 5 - Flow depth ($0 < h < 4$ m) simulated by FLO-2D after 0.25, 1, 2 and 4 hours

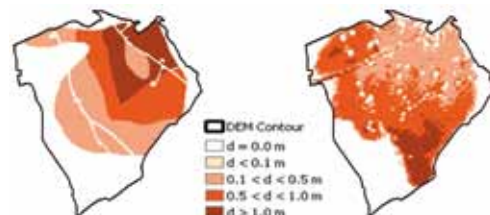


Fig. 6 - Comparison between the measured (left) and simulated (right) deposition depths

The discrepancy is resolved considering a mudflow with a 0.86 solid concentration value whose rheology corresponds to the Natural Aspen Soli with a 0.45 solid concentration value. Using roughness coefficient values $K_s = 3, 13, 30$ and $40 \text{ m}^{1/3}/\text{s}$ for buildings, wooded area, grass and roads respectively, mudflow mass after, 4 hour, has velocities lower than 0.001 m/s (Figure 5) and is assumed deposited. Figure 6 shows the comparison between the measured deposition depths and the simulated flow depths (as FLO-2D does not simulate the deposition, flow depth is considered deposition depth if velocity is less than 0.001 m/s).

The extension of the simulated area satisfactory coincides with the deposition area while the simulated sediment depth distribution is somehow reversed respect to that measured. The measured sediment depths are larger upstream and decrease downstream while the simulated sediment depths are lower upstream and increase downstream. This fact is due to the missing of a direct deposition mechanism in the FLO-2D model for which flow depths, when velocities are lower than 0.001 m/s, become larger when slope decreases, in the present case downstream.

CELL MODEL SIMULATIONS

Cell model simulations were carried out using the same input hydrograph and same inlet cells of Flo-2D simulations. The value of the conductance coefficient C was assumed constant and equal to 3 according to GREGORETTI (2000), that is about $10 \text{ m}^{1/3}/\text{s}$. Considering that coefficient C contains the rheological law the flow resistance is equivalent in the two cases. The values of parameters of the best simulation, that is, with the best agreement with measured deposits, are $K = 0.1$, $\theta_{LM} = 20^\circ$ for erosion and $\theta_{LM} = 6^\circ$ for deposition, $U_{LM-E} = 3 \text{ m/s}$, $U_{LM-D} = 1 \text{ m/s}$, $h_{ER} = 0.1 \text{ m}$ and $h_{ROUT} = 0.01 \text{ m}$. The parameters relative to the erosion are irrelevant. The value $\theta_{LM} = 6^\circ$ corresponds to bed slope angles for which solid phase of sediment debris flow begins deposition. The value of parameter K is slightly inferior to the minus value of those used for 1D simulation by Brufau *et alii* (2000): $0.2 \leq K \leq 1$. A change of h_{ROUT} in the range 0.01-0.05 m does not imply substantial modification of results. The simulation time is about 0.39 h (about 24 minutes). Figure 7 is analogous to figure 5 and shows the inundated areas and flow depth values at different times.

The routing times of Flo-2D and cell model simulation are different. This difference depends on the rheological law. Flo-2D uses a viscous flow law while cell model uses a grain-inertial flow law. The routing time of cell model simulation is more physically plausible than the routing time of Flo-2D simulation that is too large. Figure 8 shows the comparison between the measured deposit depths and those simulated by the cell model. The extension of the simulated area satisfactory coincides with the deposition area, as in the case of Flo-2D, and the simulated sediment depth distribution somehow agrees with that measured. The measured and simulated sediment depths are both larger upstream and decrease downstream. The cell model, as Flo-2D, simulates dep-

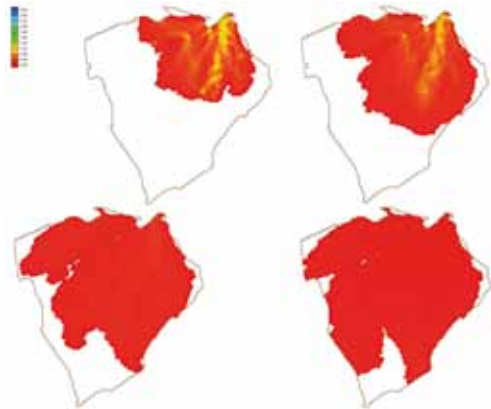


Fig. 7 - Flow depth ($0 < h < 4 \text{ m}$) simulated by cell model after 0.065, 0.13, 0.26 and 0.39 hours

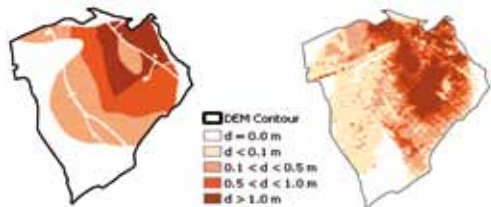


Fig. 8 - Comparison between the measured (left) and simulated (right) deposition depths

osition in the lower right corner of the basin where the debris deposits are absent. This fact could be due to the initial assumption of monophasic flow. Considering a bi-phase flow after sediments deposition, flow is largely constituted of fluid that spills out from the border of the considered basin. The monophasic assumption causes the continuous deposition until the basin border.

DISCUSSION OF THE SIMULATIONS RESULTS

The comparison of the extension of deposition area simulated by the two models with that measured is shown in Table 1.

Table 1 also shows the comparison in percentage of the value of the measured deposition depths with those simulated by the two models. The first comparison is direct and the second one is carried out verifying that the simulated value is included in a fixed interval. The measured depths have been divided in four intervals: $d < 0.1 \text{ m}$, $0.1 < d < 0.5 \text{ m}$, $0.5 < d < 1 \text{ m}$ and $d > 1.0 \text{ m}$.

Figure 9 also shows this second comparison. Inundated areas are well simulated by both the models (91% of inundated area in the case of Flo-2D and 95.9% in the case of the cell model) even if they

both predicts a larger inundated area (124 % and 139% of inundated areas respectively). Nevertheless cell model simulates more correctly the deposit depths than the Flo-2D (50.5 % against 18% of the measured area: the half of the simulated deposition depths by the cell model in the measured deposition area are correct whereas it occurs only for more than a fourth of the simulated deposition depths by Flo-2D in the measured area. Moreover as regard the total

	Flo-2D	Cell model
Percentage of measured deposition area that was simulated .	91.1	95.9
Percentage of deposition area simulated but not measured	33.2	43
Percentage of measured area with deposit depths correctly simulated	18.4	50.5
Percentage of measured area corresponding to $d > 0.5$ m with deposit depth correctly simulated	27.1	47

Tab. 1 - Comparison of the extension of measured deposition area and deposition depths with those simulated by the two models

simulated deposition area, the 36% of it is correctly simulated in the case of the cell model and the 14.5 % in the case of Flo-2D model. Considering only the area with deposit depths larger than 0.5 m, that corresponds to the 87 % of measured sediment volume, the cell model provides 47 % of deposition area correctly simulated while Flo-2D provides 27.1 % of it.

Comparing the measured deposition depths with those simulated of figure 9, it can be observed that the cell model is able to simulate right deposition depth in all the inundated area while Flo-2D model predicts the deposits only in a intermediate position. This is the reason why Flo-2D simulates correctly only the 27.4% of the area with deposits larger than 0.5 m that are located in the upper part.

This aspect can be better seen in Figure 10 where the zones with correct simulated deposit depths are shown along with zones with uncorrected simulated deposit depths, zones with measured deposit but not simulated and zones with simulated deposit but no measured. It can be observed that the blue areas corresponding to correctly simulated deposit depths are distributed on all the inundated areas in the case of the cell model while this does not occurs in the case of Flo-2D.

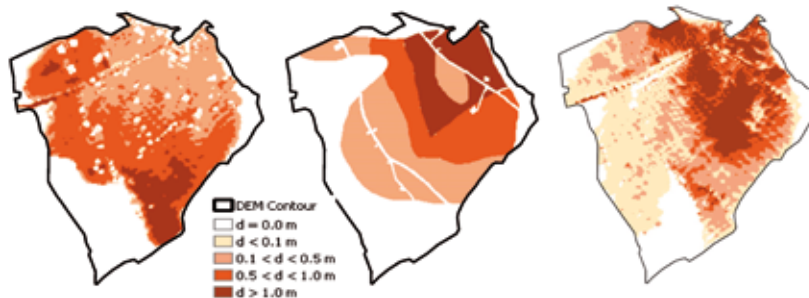


Fig. 9 - Comparison between the measured deposit depths (middle) and those simulated by Flo-2D (left) and cell model (right)

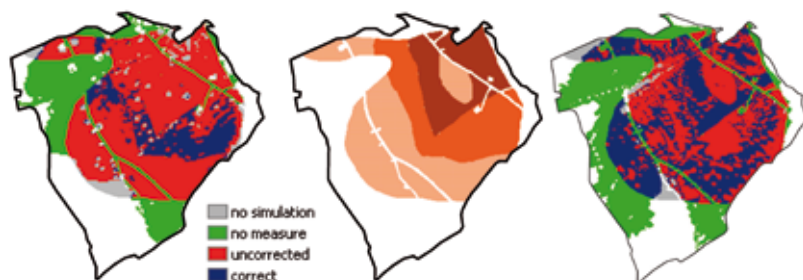


Fig. 10 - Comparison between measured and simulated deposition depths (left Flo-2D simulation, middle measured depths and right cell model simulation): gray deposition depths measured but not simulated; green deposition depths simulated but not measured; red deposition depths with simulated uncorrected values; blue deposition depths correctly simulated

	$\Delta x = 1 \text{ m}$	$\Delta x = 2 \text{ m}$	$\Delta x = 4 \text{ m}$
Percentage of measured deposition area that was simulated.	94.97	95.9	96.7
Percentage of deposition simulated but not measured.	34.8	43	46.7
Percentage of measured area with deposit depths correctly simulated	50.9	50.5	49.6
Percentage of measured area corresponding to $d > 0.5 \text{ m}$ with deposit depth correctly simulated	49	47	44

Tab. 2 - Comparison of the extension of measured deposition area and deposition depths simulated by cell model using different cell sizes

In this last case the blue areas are located in a intermediate position. These differences in the results of the two model are due to the different rheological laws implemented by the models. Flo-2D models debris flow as viscous continuous and this implies larger deposition depths in the downstream part of deposition area as it occurs in many real cases but not in the present one. Cell model that includes the rheological law in the conductance coefficient C is not subjected to any chain under this point of view. The fact that Flo-2D cannot directly simulate the deposition phase forbids the correct simulation of deposit depths in the upstream part (most of sediment of debris flow deposited just after the spilling out of the channel during the event). On this point of view, cell model appears more suitable to simulate debris flow deposition phase on a fan. Moreover the routing times of cell model are more physically realistic than those of Flo-2D when simulating the deposition phase of the debris flow occurred on Rio Lazer.

It should be added that the use of a same hydrograph can introduce some bias when comparing the results of the simulations of the two models. The correct hydrograph to be used with Flo-2D should be little lower than that of Figure 4 because the debris flow volume and the deposition volume must coincide. As the difference between the hydrograph volume and deposit volume is little it means that the use of an hydrograph with a little smaller volume does not change significantly the results of the Flo-2D simulation. The percentage of deposition area correctly simulated and the percentage of measured area with deposit depths correctly simulated should change just a bit while the simulated deposition area should decrease.

Finally some words about the influence of cell size on the simulation in the case of flow cell model. Table 2 is analogous to table 1 and compares the performance of flow cell model for three different cell size Δx : 1, 2 and 4 m.

The performance of cell model slightly increases with the decrease of cell size in the case of percentage of measured area with deposit depth larger than 0.5 m correctly simulated and percentage of deposition simulated but not measured. In the other case the differences in the performances are negligible. This leads to affirm a very slightly influence of cell size in the simulation results.

CONCLUSIONS

A cell model is proposed for simulating debris flow routing and deposition phases on a fan and design hazards maps. The simplifications at the base of the model do not strictly respect the physics of routing when considering the routing times but allow a simulation of deposition depth quite realistic. Debris flow occurred the 4th of November 1966 on Rio Lazer torrent has been simulated with satisfactory results. The same event has been simulated by the commercial model Flo-2D for comparison with a largely used model for debris flow simulation. The two simulations provide both nearly equal and different results. Both the models simulate a deposition area larger than that measured which cover the 91% of the measured area for Flo-2D and 95.9 % for the cell model. However, cell model provides a better simulation of the deposit depth about more than two times respect to Flo-2D (50.5 % against 18% of measured area). Moreover, the correctly simulated deposition depths are distributed all over the deposition area while in the case of Flo-2D simulation, they are grouped in a unique zone of it. This fact is due to the missing of direct deposit mechanism in the Flo-2D model that indirectly simulates it when velocity reduces to the order of 0.001 m/s. This obliges the use of viscous flow, a priori excluding the granular inertial flow, with large routing times. On this point of view, cell model appears more suitable than Flo-2D for simulating debris flow. It must be added that Flo-2D, due to the viscous flow rheological law should better simulate the extension of inundated areas. For a better comparison the two models should be both tested in cases where the deposition depths are larger on the downstream part of deposits of occurred debris flows.

ACKNOWLEDGEMENTS

This research was financially supported by the University of Padova grant ex60%, the Italian Ministry of Education and Research grant PRIN 2007 and European grant PARAmount (imProved Accessibility: Reliability and security of Alpine transport infrastructure related to mountainous hazards in a changing climate), within the Alpine Space Programme 2007-2013.

The writers wishes to thank the reviewers for they useful comments.

NOTATIONS

C = conductance coefficient;

A = cell area;

h_i = flow depth of cell i ;

h_{ER} = minimum flow depth for erosion;

h_{ROUT} = minimum flow depth for routing;

K = empirical constant;

K_S = roughness coefficient;

$i_{b,i}$ = bed erosion/deposition velocity of cell i ;

$Q_{i,k}$ = discharge exchanged between cell i and k ;

$s_{i,k}$ = weighting function;

$U_{i,k}$ = flow velocity from cell i to cell k ;

U_{LIM-D} = upper limit velocity for deposition;

U_{LIM-E} = inferior limit velocity for erosion;

V_i = flow volume in cell i ;

$w_{i,k}$ = weighting function;

z_i = bottom elevation of cell i ;

Δt = time step;

Δx = cell size;

$\theta_{i,k}$ = the angle respect to the horizontal between the line joining the centres of cell i and k ;

$\theta_{i,k}$ = adopted angle for computing erosion and deposition;

θ_{LIM-D} = upper limit angle for deposition;

θ_{LIM-E} = inferior limit angle for erosion.

REFERENCES

- ARMANINI A., FRACCAROLLO L. & ROSATTI G. (2009) - *Two-dimensional simulation of debris flows in erodible channels*, Computers & Geosciences, **35**(5): 993-1006.
- BERTI M & SIMONI A. (2007) - *Prediction of debris flow inundation areas using empirical mobility relationships*. Geomorphology, **90**: 144-161.
- BRUFAU P., GARCIA-NAVARRO P., GHILARDI P., NATALE L. & SAVI F. (2000) - *1-D mathematical modelling of debris flow*. Journal of Hydraulic Research, **38**(6): 435-446.
- CHEN J., ARLEEN A.H. & URBANO L.D. (2009) - *A GIS-based model for urban flood inundation*. Journal of hydrology, **373**: 184-192.
- D'AMBROSIO D., DI GREGORIO S., IOVINE G., LUPIANO V., RONGO R. & SPATARO W. (2003) - *First simulation of the Sarno debris flows through Cellular Automata modelling*. Geomorphology, **54**: 91-117.
- DEANGELI C. (2008) - *Laboratory granular flows generated by slope failures*. Rock Mechanics and Rock Engineering, **41**(1): 199-217.
- EGASHIRA S. & ASHIDA K. (1987) - *Sediment transport in steep slope flumes*. Proc. of Roc Japan Joint Seminar on Water Resources.
- GREGORETH C. (2000) - *Estimation of the maximum velocity of a surge of debris flow propagating along an open channel*. Interpraevent2000 - Villach 26-30 June, 99-108.
- GRISWOLD J.P. & IVERSON R.M. (2008) - *Mobility Statistics and Automated Hazard Mapping for Debris-flows and Rock Avalanches*, US Geological Survey Scientific Investigation Report 5276, US Geological Survey: Reston, VA; 59.
- GRUBER S. (2007) - *A mass-conserving fast algorithm to parametrize gravitational transport and deposition using digital elevation models*. Water Resources Research, **43**.
- IVERSON R.M., SCHILLING S.P. & VALLANCE J.W. (1998) - *Objective delineation of lahar-inundation hazard zones*. GSA Bulletin **110**(8): 972-984.
- JAIN M.K., KOTHYARI U.C. & RANGA RAJU K.G. (2005) - *GIS based distributed model for soil erosion and rate of sediment outflow from catchments*. Journal of Hydraulic Engineering, ASCE, **131**, 9: 755-769.
- MASCARENHAS F.C.B. & MIGUEZ M.G. (2002) - *Urban flood control through a mathematical cell model*. Water International, IWRA, 2002, **27**(2): 208-218.
- MIGUEZ M.G., MASCARENHAS F.C.B., CANEDO DE MAGALHAES L.P. & VELLOZO D'ALTERIO C.F. (2009) - *Plannig and design of urban flood control measures: assessing effect combination*. Journal of Urban Planning and Development, ASCE, **135**(3): 100-109.
- O'BRIEN J.S. & JULIEN P.Y. (1985) - *Physical processes of hyperconcentrated sediment flows*. Proc. of the ASCE Conference on the Delineation on Landslides, Floods and Debris Flow hazards in Utah. Utah Water Research Laboratory, Series

UWRL/g85/03: 260-279.

- PASTOR M., HADDAD B., SORBINO G. & CUOMO S. & DEMPTRIC V. A. (2008) - *A depth integrated-coupled SPH model for flow like landslides and related phenomena*. International Journal for Numerical and Analytical Methods in Geomechanics.
- RICKENMANN D. (2005) - *Runout prediction methods*. In *Debris-Flow Hazards and Related Phenomena*, JAKOB M. & HUNGR O. (EDS). Praxis Springer: Berlin Heidelberg: 305-324.
- RICCARDI G.A. (1997) - *The mathematical modeling of flood propagation for the delineation of flood risk zones*. IAHS publication, **240**: 355-363.
- SCHEIDL C. & RICKENMANN D. (2010) - *Empirical prediction of debris-flow mobility and deposition on fans*. Earth and Surface Process Landform, **35**: 157-173.
- ROSATTI G.A. & FRACCAROLLO L. (2007) - *Simulation of debris flow in erodible channels*. Proceedings of the 32nd Congress of IAHR, Venice, Italy.
- SEGRE E. & DEANGELI C. (1995) - *Cellular automaton for realistic modeling of landslides*. Nonlinear Processes in Geophysics, **2**: 1-15
- SEMINARA G. & TUBINO M. (1993) - *Debris flows: meccanica, controllo e previsione*. Monografia G.N.D.C.I., 1993.
- TAKANASHI K., MIZUYAMA T. & NAKANO Y. (2007) - *A method for delineating restricted hazard areas due to debris flows*. Proceedings of the 4th International Congress on Debris-Flow Hazards Mitigation, Chengdu 10-13 September: 471-478.
- TSUBAKI (1972) - *Keikoku taiseki dosha no ryndo*. XXVII Japanese National Congress on Civil Engineering (in Japanese).
- ZANOBETTI D.H., PREISSMAN A., & CUNGE J.A. (1970) - *Mekong Delta mathematical program construction*. Journal of Waterways and Harbour Division, ASCE, **96**(2): 181-199.